Atomic Parity Violation in Ytterbium

K. Tsigutkin, D. Dounas-Frazer, A. Family, and D. Budker

http://budker.berkeley.edu

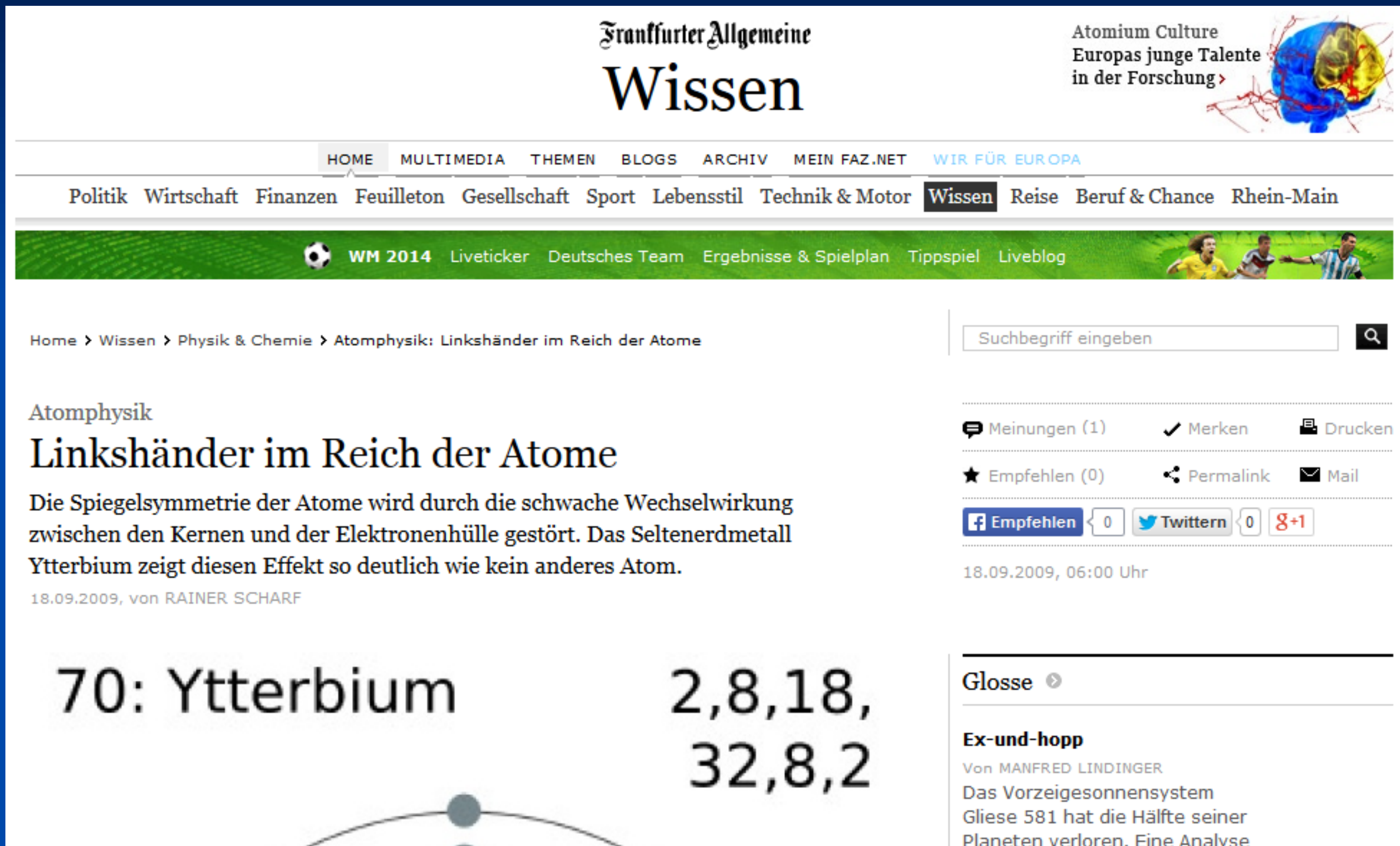

Frankfurter Allgemeine
Wissen

Atomium Culture
Europas junge Talente
in der Forschung ›

HOME MULTIMEDIA THEMEN BLOGS ARCHIV MEIN FAZ.NET WIR FÜR EUROPA

Politik Wirtschaft Finanzen Feuilleton Gesellschaft Sport Lebensstil Technik & Motor Wissen Reise Beruf & Chance Rhein-Main

WM 2014 Liveticker Deutsches Team Ergebnisse & Spielplan Tippspiel Liveblog

Home › Wissen › Physik & Chemie › Atomphysik: Linkshänder im Reich der Atome

Suchbegriff eingeben

Atomphysik

Linkshänder im Reich der Atome

Die Spiegelsymmetrie der Atome wird durch die schwache Wechselwirkung zwischen den Kernen und der Elektronenhülle gestört. Das Seltenerdmetall Ytterbium zeigt diesen Effekt so deutlich wie kein anderes Atom.

18.09.2009, von RAINER SCHARF

70: Ytterbium 2,8,18,32,8,2

Meinungen (1) Merken Drucken
Empfehlen (0) Permalink Mail
Empfehlen 0 Twittern 0 g+1

18.09.2009, 06:00 Uhr

Glosse

Ex-und-hopp

Von MANFRED LINDINGER

Das Vorzeigesonnensystem Gliese 581 hat die Hälfte seiner Planeten verloren. Eine Analyse

Atomic PV: important landmarks

- 1959 **Ya. B. Zel'dovich:** APV (Neutr. Current) $\Rightarrow$ Opt. Rotation in atoms
- 1974 **M.-A. & C. Bouchiat** Z^3 enhancement $\Rightarrow$ APV observable in **heavy** atoms
- 1978-9 **Novosibirsk, Berkeley** discovery of APV in OR(**Bi**) and Stark-interf.(**Tl**)
- 1995 **Boulder, Oxford, Seattle, Paris** APV measured to 1-2% in Cs, Tl, Bi, Pb
- 1997 **Boulder** 0.35% measurement, discovery of anapole moment

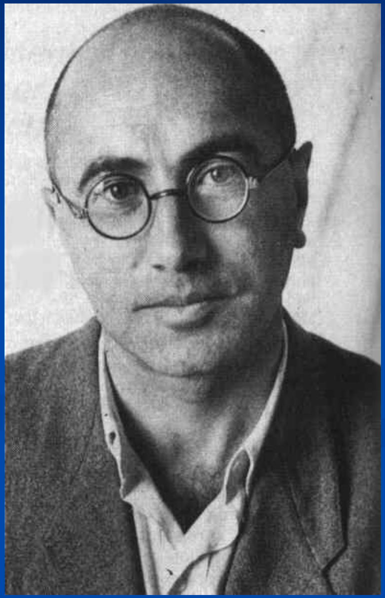

Prof. Ya. B. Zel'dovich

Parity transformation

$$P: \begin{pmatrix} x \\ y \\ z \end{pmatrix} \mapsto \begin{pmatrix} -x \\ -y \\ -z \end{pmatrix}$$

Parity transformation is a **point reflection**.

$\det(P) = -1$

Classification of classical variables:

Rotational transformation

Parity transformation

Variables
- **Scalars**
  - **Scalars (P=1): Mass, Energy, Time …**
  - **Pseudoscalars (P=-1): Helicity …**
- **Vectors**
  - **Vectors (P=-1): Linear momentum, E-field, Force …**
  - **Pseudovectors (P=1): Angular momentum, B-field …**

Two frontiers in the search

Collider experiments (pp, e^+e^-, etc) at higher energies ($E >> M_Z$)

High energy physics

Indirect searches at lower energies ($E < M_Z$) but high precision

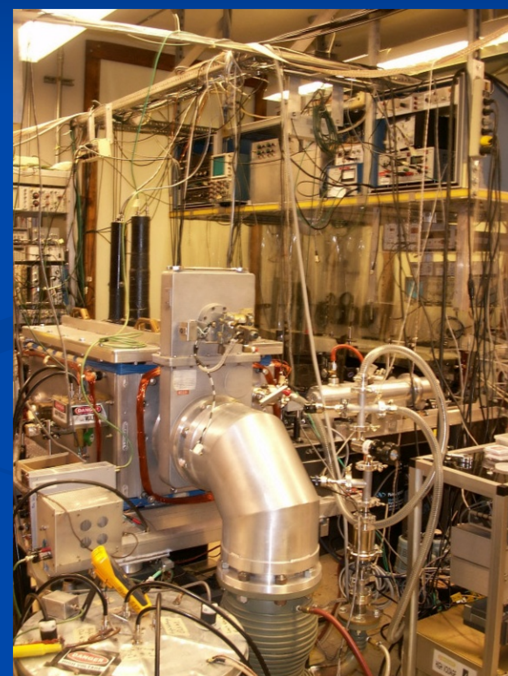

Particle, nuclear & atomic physics

Sources of parity violation in atoms

Z^0-exchange between e and nucleus

$\Rightarrow$ P-violating, T-conserving product of axial and vector currents

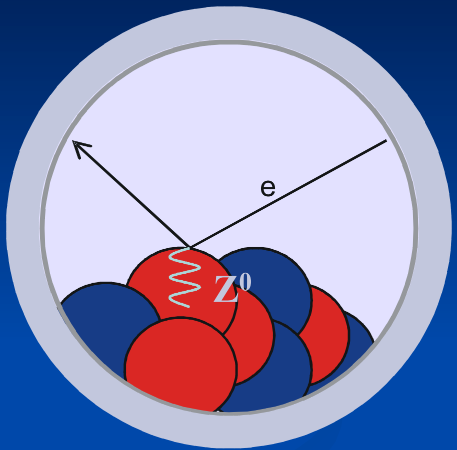

$$\hat{h} = -\frac{G}{\sqrt{2}} \sum_N \left[C_{1N} \boxed{\bar{e}\gamma_\mu\gamma_5 e} \boxed{\bar{N}\gamma_\mu N} + C_{2N} \boxed{\bar{e}\gamma_\mu e} \boxed{\bar{N}\gamma_\mu\gamma_5 N} \right]$$

C_{1n} is by a factor of 10 larger than C_{1p}, C_{2N} leading to a dominance of the time-like nuclear spin-independent interaction (A_e, V_N)

A contribution to APV due to Z^0 exchange between electrons is suppressed by a factor ~1000 for heavy atoms.

Nuclear Spin-Independent (NSI) electron-nucleon interaction

NSI Hamiltonian in non-relativistic limit assuming equal proton and neutron densities $\rho(r)$ in the nucleus:

$$\hat{h}_W = -\frac{G}{2\sqrt{2}} Q_W \gamma_5 \rho(r)$$

The nuclear weak charge Q_W to the lowest order in the electroweak interaction is

$$Q_W = -N + Z(1 - 4\sin^2\theta_W) \approx -N$$

$$\sin^2\theta_W = 1 - \left(\frac{M_W}{M_Z}\right)^2$$

The nuclear weak charge is protected from strong-interaction effects by conservation of the nuclear vector current. **Thus, APV measurements allows for extracting weak couplings of the quarks and for searching for a new physics beyond SM**

- NSI interaction gives the largest PV effect compared to other mechanisms
- PV interaction is a pseudo-scalar $\Rightarrow$ mixes only electron states of same angular momentum

NSI interaction and particle physics implications

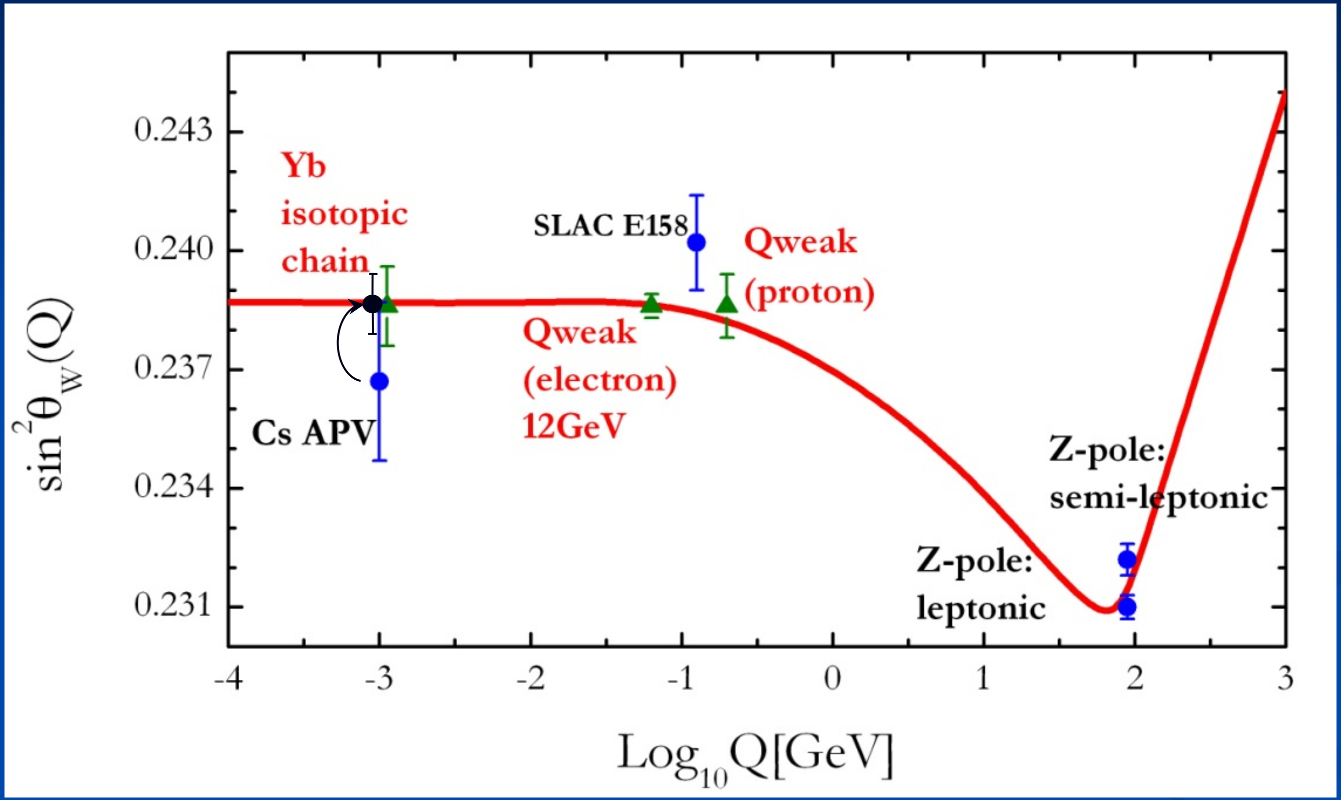

APV utilizes low-energy system and gives an access to the weak mixing angle, $\mathrm{Sin}^2(\theta_W)$, at low-momentum transfer.

- S. G. Porsev, K. Beloy, and A. Derevianko, PRL 2009
- J.L. Rosner, PRD 1999
- V.A. Dzuba, V.V. Flambaum, and O.P. Sushkov, PRA 1997
- J. Erler and P. Langacker, Ph.Lett. B 1999

Isotope ratios and neutron distribution

The atomic theory errors can be excluded by taking ratios of APV measurements along an isotopic chain. While the atomic structure cancels in the isotope ratios, there is an enhanced sensitivity to the neutron distribution $\rho_n(r)$.

$$A_{PV} = \xi_{atomic}(Q_W + Q_W^{nuc})$$

$$Q_W^{nuc} = -N(q_n - 1) + Z(1 - 4\sin^2\theta_W)(q_p - 1)$$

$$q_n = \int \rho_n(r) f(r) \mathrm{d}^3 r, \quad q_p = \int \rho_p(r) f(r) \mathrm{d}^3 r$$

f(r) is the variation of the electron wave functions inside the nucleus normalized to f(0)=1.

$$R \equiv \frac{A_{PV}(N')}{A_{PV}(N)} \approx \frac{Q_W(N')}{Q_W(N)} \left[1 + \Delta q_n\right]$$

$$\Delta q_n \equiv q_n - q_n'$$

R is sensitive to the difference in the neutron distributions.

Amplitude interference: the trick for observing weak interaction in atoms

$\mathbf{h_{NSI}}$ mixes $\mathbf{s_{1/2}}$ and $\mathbf{p_{1/2}}$ states of valence electron $\Rightarrow$
$\mathbf{A_{PV}}$ of dipole-forbidden transition.
If $\mathbf{A_{PC}}$ is also induced, the amplitudes interfere.

$$R \propto \left|A_{PC} + A_{PV}\right|^2 \cong A_{PC}^2 + 2A_{PC}A_{PV} + o(A_{PV}^2)$$

Interference

E-field ➡ Stark-effect ➡ E1 PC-amplitude ∝ E ➡ E1-PV interference term is odd in E

Reversing E-field changes transition rate
Transition rate ∝ $\mathbf{A_{PV}A_{Stark}}$

Observing APV in Yb

Proposed by D. DeMille, PRL 1995

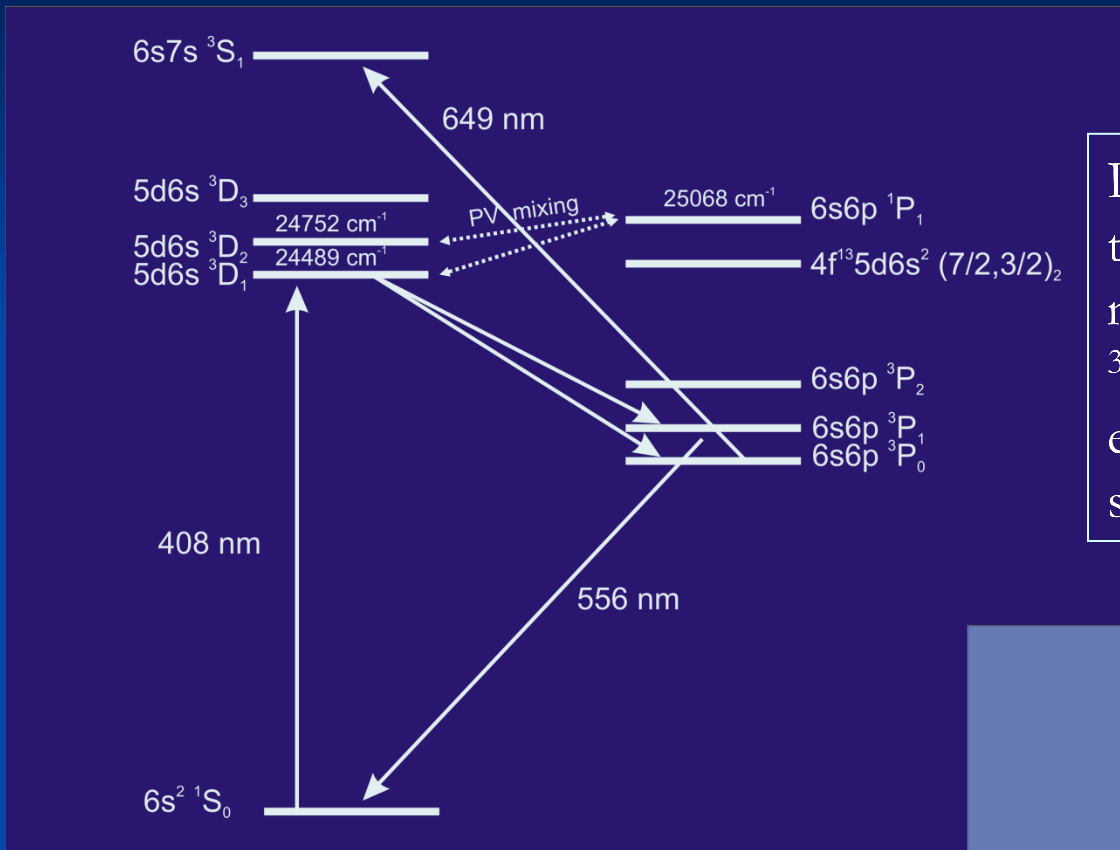

Pumping rates of the 408-nm transition are detected by measuring the population of the $^3P_0$ state, where 65% of the atoms excited to the $^3D_1$ state decay spontaneously.

The population of 6s6p $^3P_0$ metastable level is probed by pumping the 6s6p $^3P_0$ - 6s7s $^3S_1$ 649 nm transition.

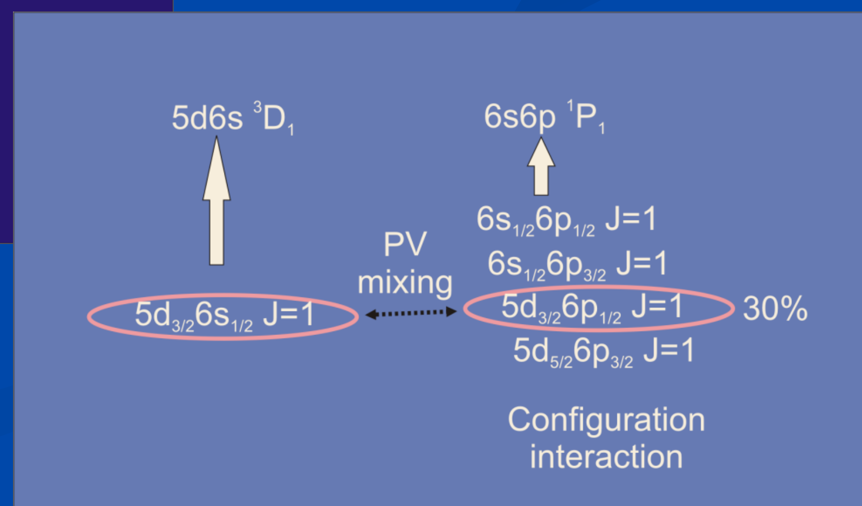

PV effect: line-shape signature

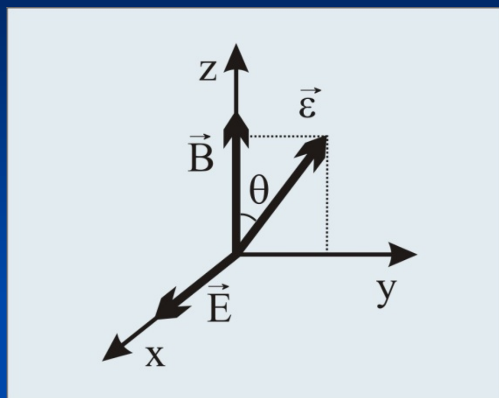

$$\vec{E} = E\,\hat{x}$$

$$\vec{\varepsilon} = \varepsilon\,(\sin\theta\,\hat{y} + \cos\theta\,\hat{z})$$

$$R_0 = 4\varepsilon^2(\beta^2E^2\sin^2\theta + 2E\,\beta\varsigma\sin\theta\cos\theta)$$

$$R_{\pm1} = 2\varepsilon^2(\beta^2E^2\cos^2\theta - 2E\,\beta\varsigma\sin\theta\cos\theta)$$

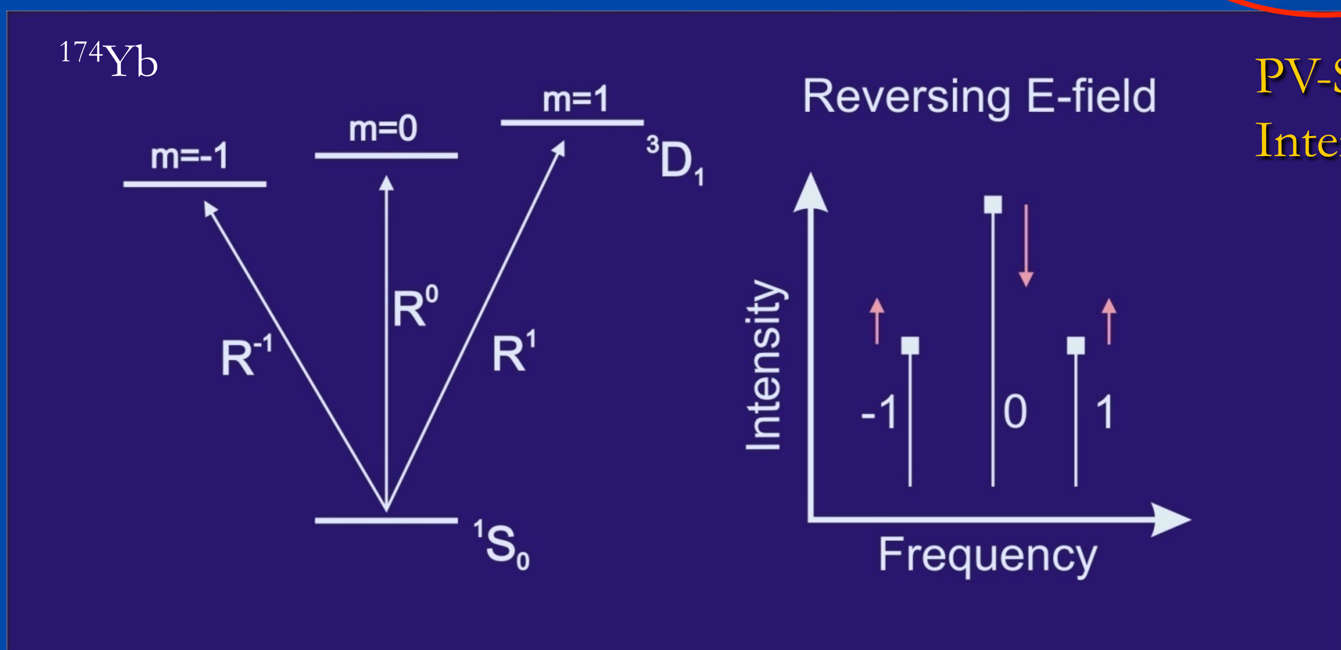

PV-Stark Interference

Experimental setup

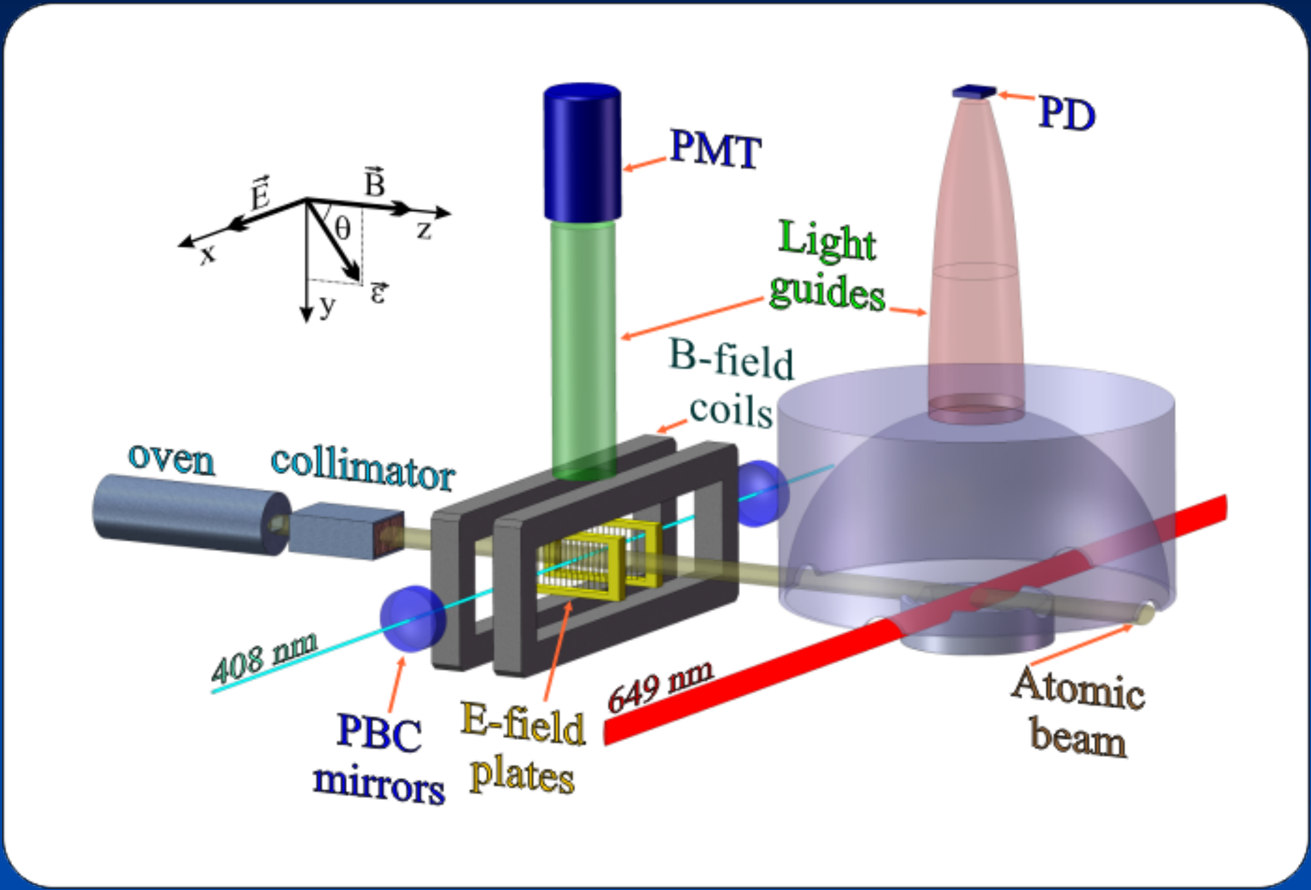

Light collection efficiency:

Interaction region: ~0.2% (556 nm)

Detection region: ~25%

Yb density in the beam ~10^{10} cm^{-3}
E-field up to 15 kV/cm, spatial homogeneity 99%
Reversible B-field up to 100 G, homogeneity 99%

Schematic of the optical system

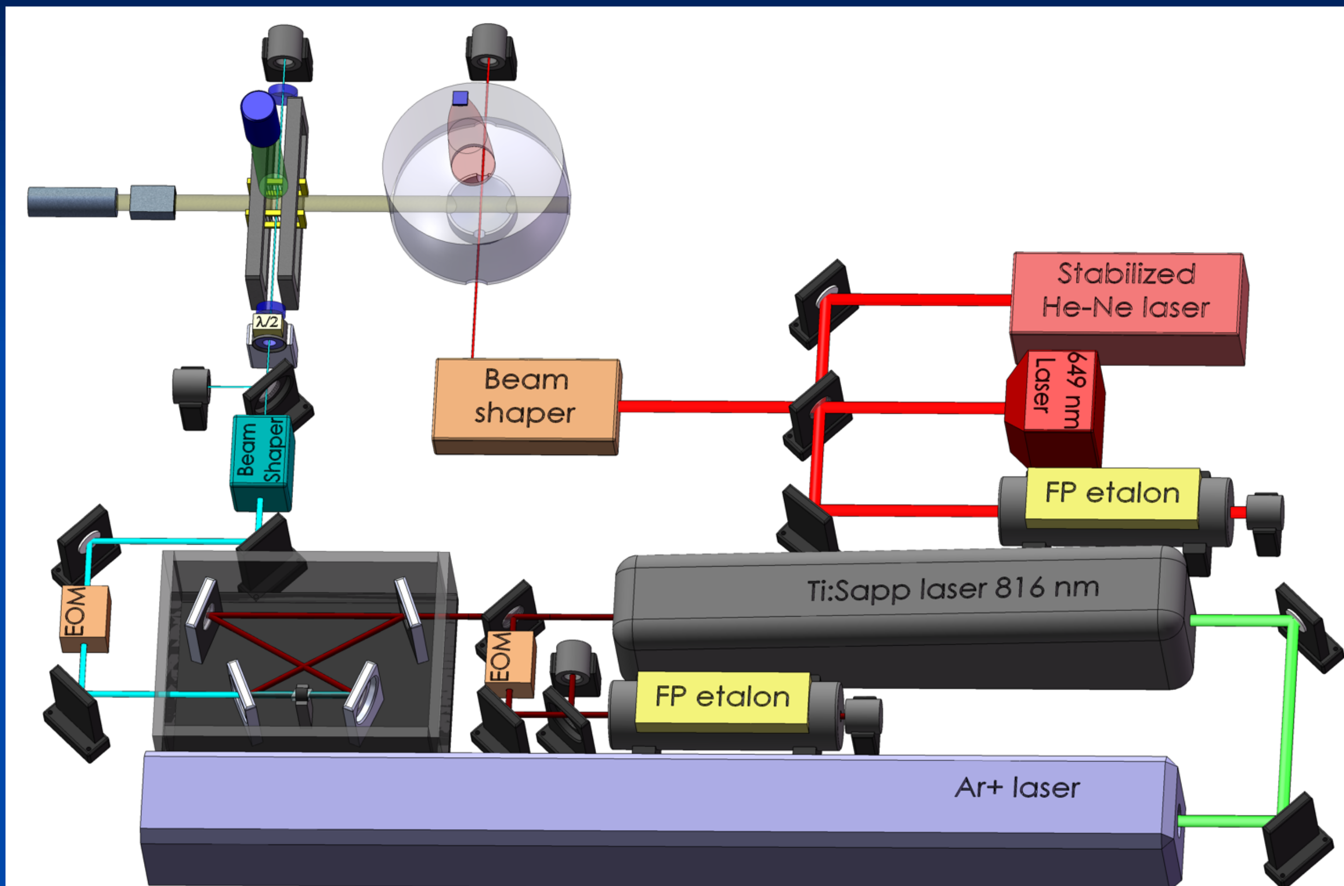

PBC:
Asymmetric design
Finesse 17000
Power 20 W
Locking:
Pound-Drever-Hall technique

Light powers:
Ar^+: 12W; Ti:Sapp (816 nm): 1W; Doubler (408 nm): 50 mW

Fast (70 Hz) E-modulation scheme

to avoid low-frequency noise and drift issues

E-field modulation $$E \rightarrow E_{\mathrm{dc}} + E_0 \cos(\omega t)$$

Transition rates $$R_{\mathrm{M}} = R_{\mathrm{M}}^{[0]} + R_{\mathrm{M}}^{[1]} \cos(\omega t) + R_{\mathrm{M}}^{[2]} \cos(2\omega t)$$

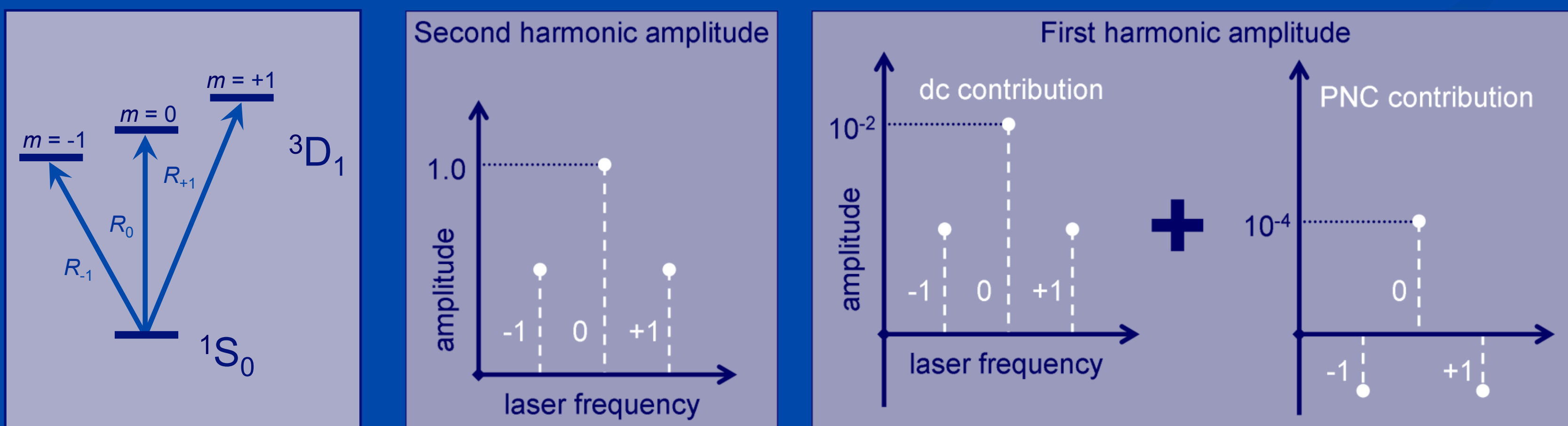

PV-asymmetry: $$K = \frac{R_{-1}^{[1]}}{R_{-1}^{[2]}} + \frac{R_{+1}^{[1]}}{R_{+1}^{[2]}} - 2\frac{R_0^{[1]}}{R_0^{[2]}} = \frac{16\ \varsigma}{\beta E_0}$$

Fast E-modulation scheme: Profiles

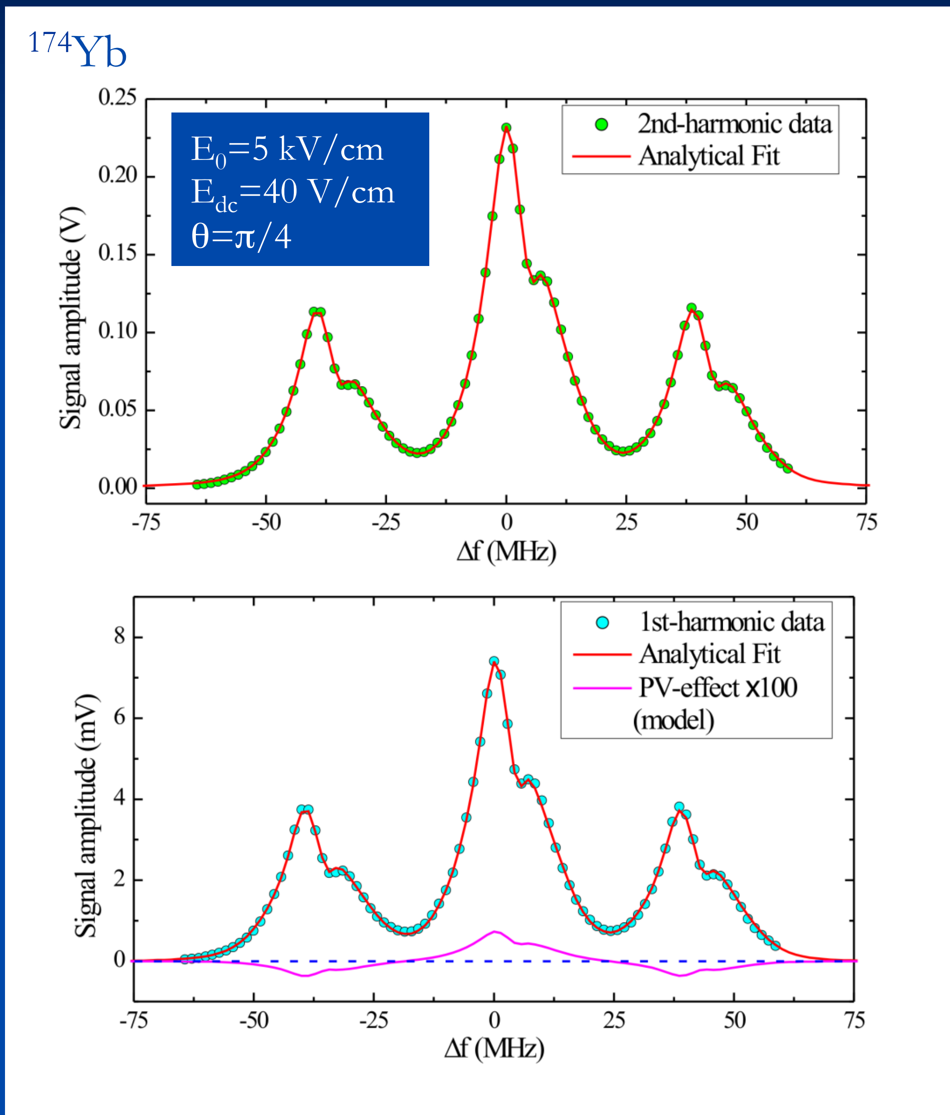

Effective integration time: 10 s p-p

Shot noise limited SNR with respect to PV signal ~ $2/\sqrt{\tau(s)}$

⇒ 0.1% accuracy in 70 hours

- Lineshape scan: 20 s
- E-field reversal: 14 ms (70 Hz)
- B-field reversal: 20 minutes
- Polarization angle: 10 minutes
- E-field magnitude
- B-field magnitude
- Angle magnitude

PV Amplitude: Current results

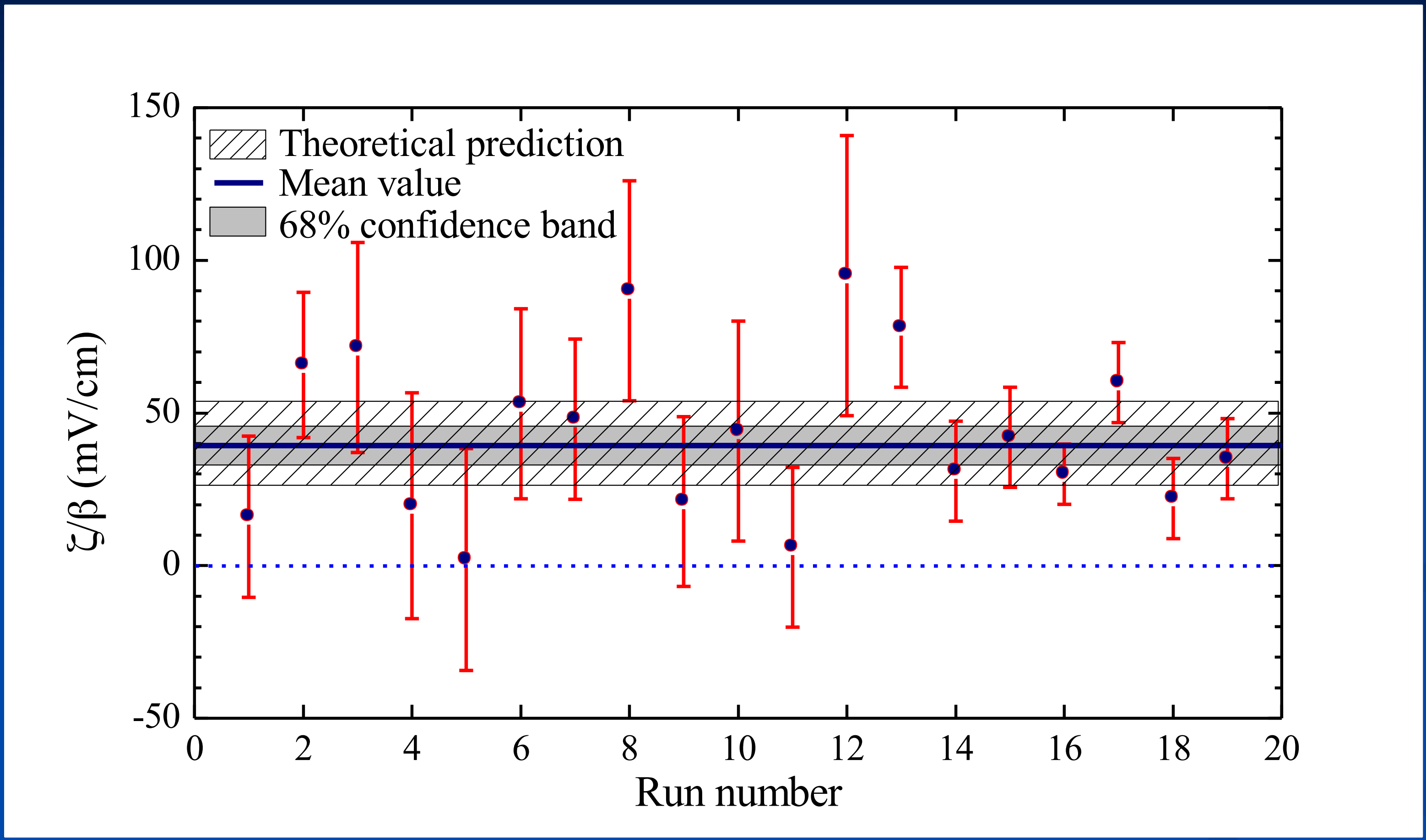

$\zeta/\beta = 39(4)_{stat.}(3)_{syst.}$ mV/cm $\Rightarrow |\zeta| = 8.7 \pm 1.4 \times 10^{-10}\ ea_0$

Accuracy is affected by HV amplifier noise, fluctuations of stray fields, and laser drifts $\rightarrow$ to be improved

Summary

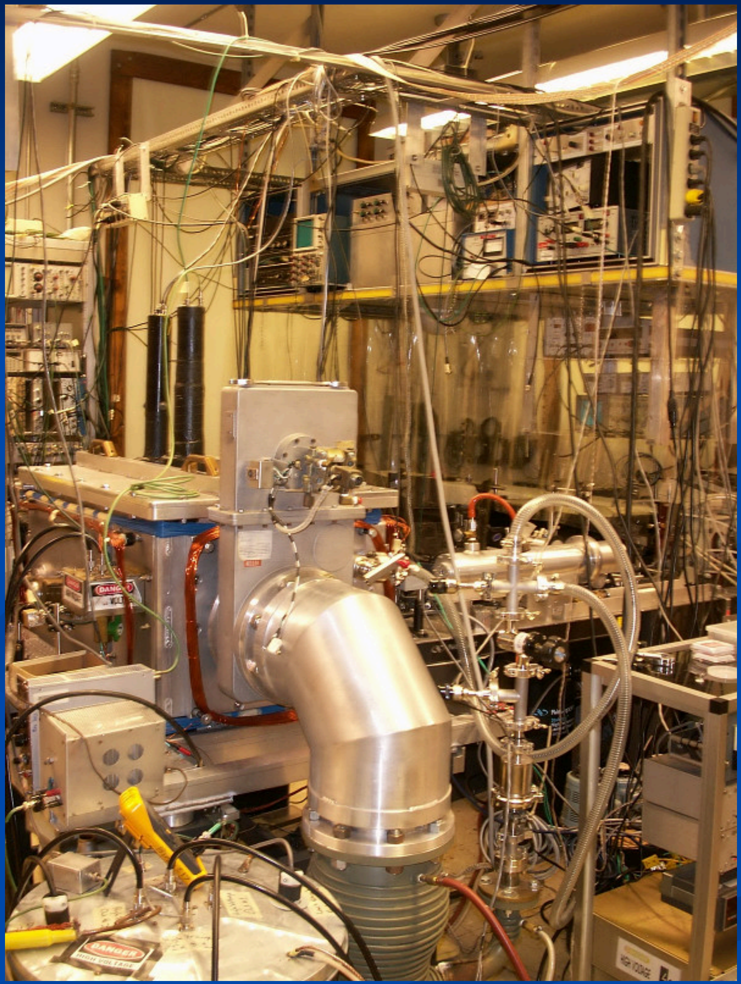

<u>Completed Work</u>

- ✓ Lifetime Measurements
- ✓ General Spectroscopy (hyperfine shifts, isotope shifts)
- ✓ dc Stark Shift Measurements
- ✓ Stark-Induced Amplitude (β): 2 independent measurements
- ✓ M1 Measurement (Stark-M1 interference)
- ✓ ac Stark shifts measured
- ✓ Verification of PV enhancement

<u>And then…</u>

- ➢ PV in a string of even isotopes; **neutron distributions**
- ➢ PV in odd isotopes: NSD PV, **Anapole Moments** …

Statistical noise

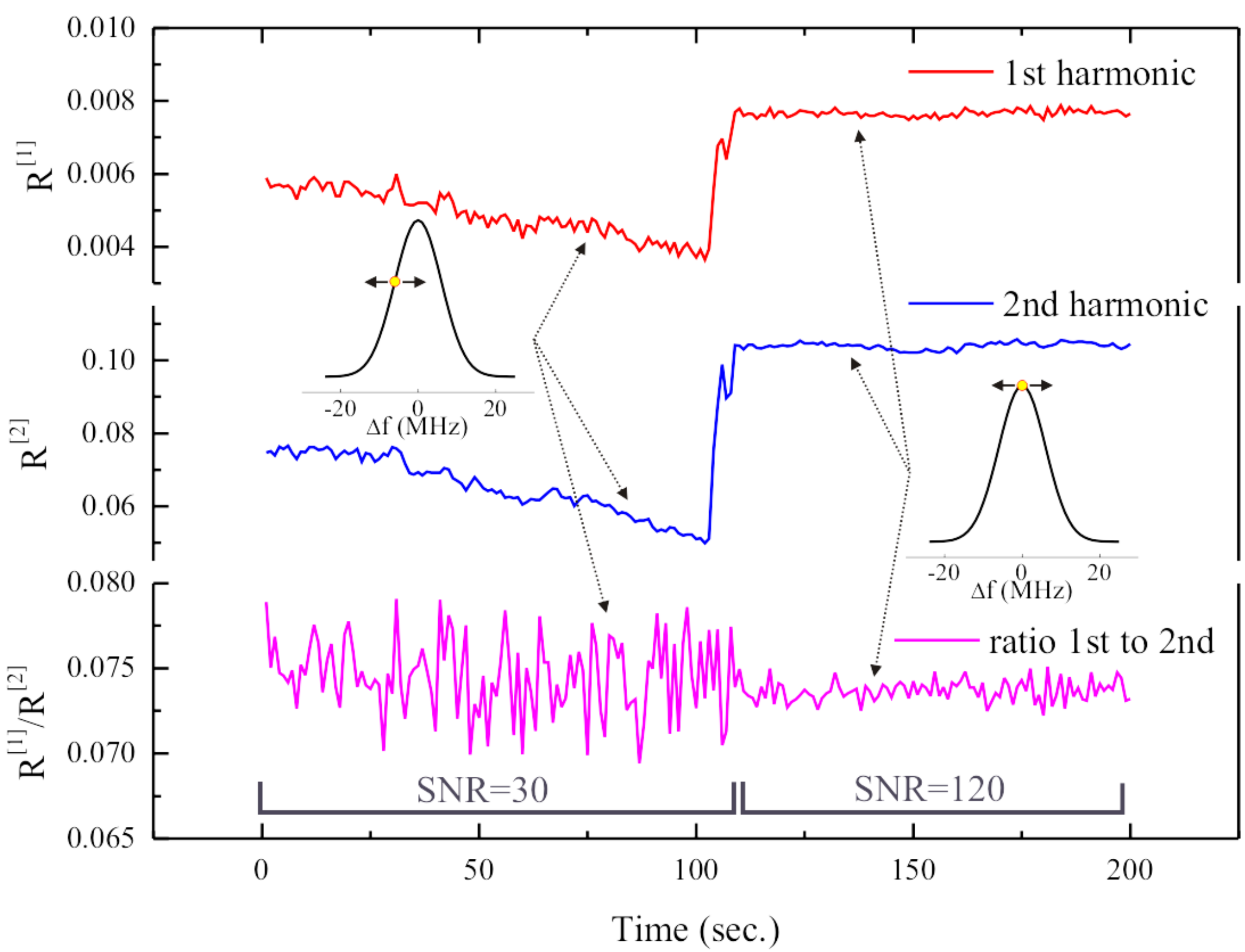

Fast E-modulation scheme: Systematics

E- and B-field imperfection:

$$\mathrm{E} = \tilde{\mathrm{E}} + \mathrm{E}'$$

$$\tilde{\mathrm{E}} = (\tilde{\mathrm{E}}_0 \hat{\mathrm{x}} + \tilde{\mathrm{e}}_y \hat{\mathrm{y}} + \tilde{\mathrm{e}}_z \hat{\mathrm{z}}) \cos(\omega \mathrm{t})$$

$$\mathrm{E}' = (\mathrm{E}_{dc} \hat{\mathrm{x}} + \mathrm{e}_y \hat{\mathrm{y}} + \mathrm{e}_z \hat{\mathrm{z}})$$

$$\mathrm{B} = \tilde{\mathrm{B}} + \mathrm{B}'$$

$$\tilde{\mathrm{B}} = (\tilde{\mathrm{b}}_x \hat{\mathrm{x}} + \tilde{\mathrm{b}}_y \hat{\mathrm{y}} + \mathrm{B} \hat{\mathrm{z}})$$

$$\mathrm{B}' = (\mathrm{b}'_x \hat{\mathrm{x}} + \mathrm{b}'_y \hat{\mathrm{y}} + \mathrm{b}'_z \hat{\mathrm{z}})$$

Light polarization now includes a small ellipticity:

$$\vec{\varepsilon} = \varepsilon \;(\hat{\mathrm{y}} \sin\theta + \hat{\mathrm{z}}\; e^{i\phi} \cos\theta)$$

Residual M1 transition:

$$\mathrm{A}_{\mathrm{M}}^{(\mathrm{M1})} = \mathrm{M1}\;(-1)^{\mathrm{M}} \left(\delta \vec{\mathrm{k}} \times \vec{\varepsilon}\right)_{\text{-M}}$$

Normalized-rate modulation amplitudes include additional terms:

$$\frac{R_{\mathrm{M}}^{[1]}}{R_{\mathrm{M}}^{[2]}} = r_{\mathrm{M}}^{(\mathrm{Stark})} + r_{\mathrm{M}}^{(\mathrm{PV})} + r_{\mathrm{M}}^{(\mathrm{M1})} + r_{\mathrm{M}}^{(\phi)}$$

M1- and ϕ-contribution

TABLE I: Lowest-order terms contributing to the normalized transition-rate modulation amplitudes r_M.

	$r_M^{(\mathrm{APV})}$	$r_M^{(\mathrm{M1})}$	$r_M^{(\phi)}$
$M=0$	$+\dfrac{4\,\zeta\cot\theta}{\beta\tilde{E}_0}$	0	0
$M=-1$	$-\dfrac{4\,\zeta\tan\theta}{\beta\tilde{E}_0}$	$+\dfrac{4\,\delta k\,\mathcal{M}(\tilde{e}_y-\tilde{e}_z\tan\theta)}{\beta\tilde{E}_0^2}$	$+\dfrac{4\,e_z\phi\tan\theta}{\tilde{E}_0}$
$M=+1$	$-\dfrac{4\,\zeta\tan\theta}{\beta\tilde{E}_0}$	$-\dfrac{4\,\delta k\,\mathcal{M}(\tilde{e}_y-\tilde{e}_z\tan\theta)}{\beta\tilde{E}_0^2}$	$-\dfrac{4\,e_z\phi\tan\theta}{\tilde{E}_0}$

$$K=\frac{R_{-1}^{[1]}}{R_{-1}^{[2]}}+\frac{R_{+1}^{[1]}}{R_{+1}^{[2]}}-2\frac{R_{0}^{[1]}}{R_{0}^{[2]}}=\frac{16\ \varsigma}{\beta E_0}$$

Stark contribution

$$\begin{bmatrix} \mathcal{K}_1 \\ \mathcal{K}_2 \\ \mathcal{K}_3 \\ \mathcal{K}_4 \end{bmatrix} = \frac{1}{4} \begin{bmatrix} -1 & -1 & +1 & +1 \\ -1 & +1 & +1 & -1 \\ +1 & -1 & +1 & -1 \\ +1 & +1 & +1 & +1 \end{bmatrix} \cdot \begin{bmatrix} \mathcal{K}(+B,+\theta) \\ \mathcal{K}(-B,+\theta) \\ \mathcal{K}(+B,-\theta) \\ \mathcal{K}(-B,-\theta) \end{bmatrix}$$

TABLE II: List of the lowest-order terms contributing to the asymmetry $\mathcal{K}$ for $|\theta| = \pi/4$ sorted with respect to their response to the reversals. $\mathcal{K}_4$ corresponding to a rather long list of terms that are invariant with respect to all reversals, is not shown in the table.

$\mathcal{K}_1$	$\mathcal{K}_2$	$\mathcal{K}_3$
$\frac{8(\tilde{e}_y e_z + \tilde{e}_z e_y)}{\tilde{E}_0^2} + \frac{16\tilde{b}_x e_y}{B\tilde{E}_0} + \frac{16\zeta}{\beta\tilde{E}_0}$	$\frac{16 b'_x e_y}{B\tilde{E}_0}$	$\frac{16 b'_x e_z}{B\tilde{E}_0}$

Stark contribution measurements

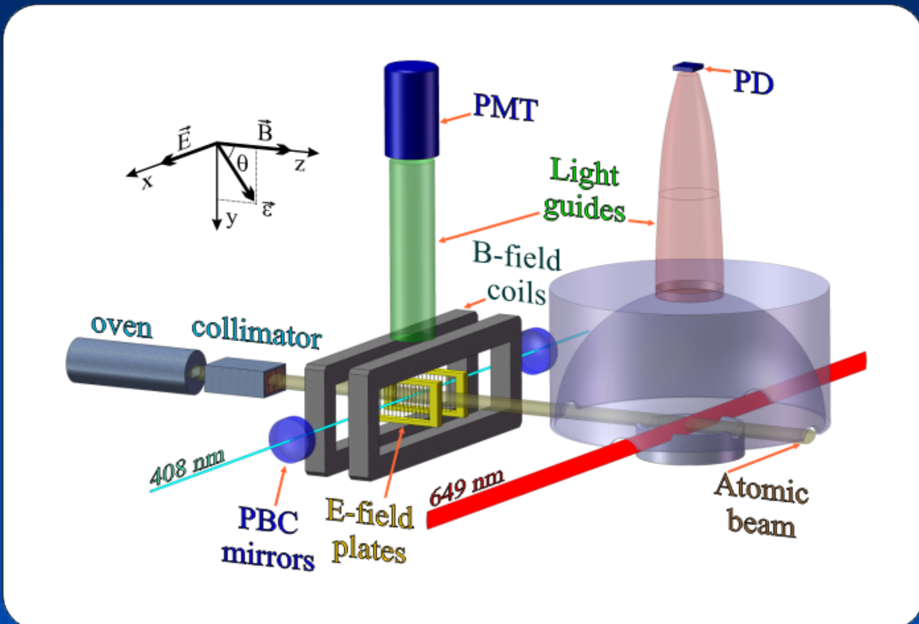

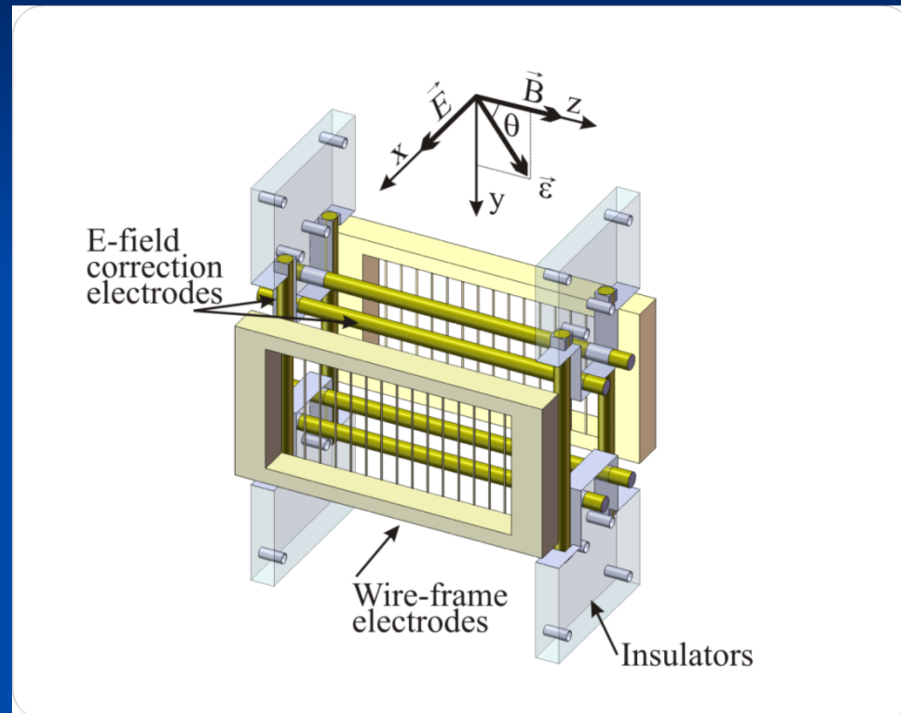

$$e_y\left(\frac{\tilde{e}_z}{2\tilde{E}_0}+\frac{b_x}{B}\right)+e_z\frac{\tilde{e}_y}{2\tilde{E}_0}=-2.6\ (1.6)_{\text{stat}}(1.5)_{\text{syst}}\ \text{mV/cm}$$

Error budget

$$\frac{\varsigma}{\beta} = 39\ (4)_{\text{stat}}(3)_{\text{syst}}\ \text{mV/cm}$$

TABLE IV: List of factors contributing to the systematic uncertainty of the PV parameter, ζ/β.

Factor	**Uncertainty (%)**
$\tilde{E}$ value:	
geometry	5
numerical modeling	3
E-field imperfections	5
Phase mixing	0.5
Other	1
Total (in quadrature)	**8**

Problems

- Photo-induced PBC mirror degradation in vacuum
- Fields imperfection
- Laser stability

Power-buildup cavity design and characterization: schematic

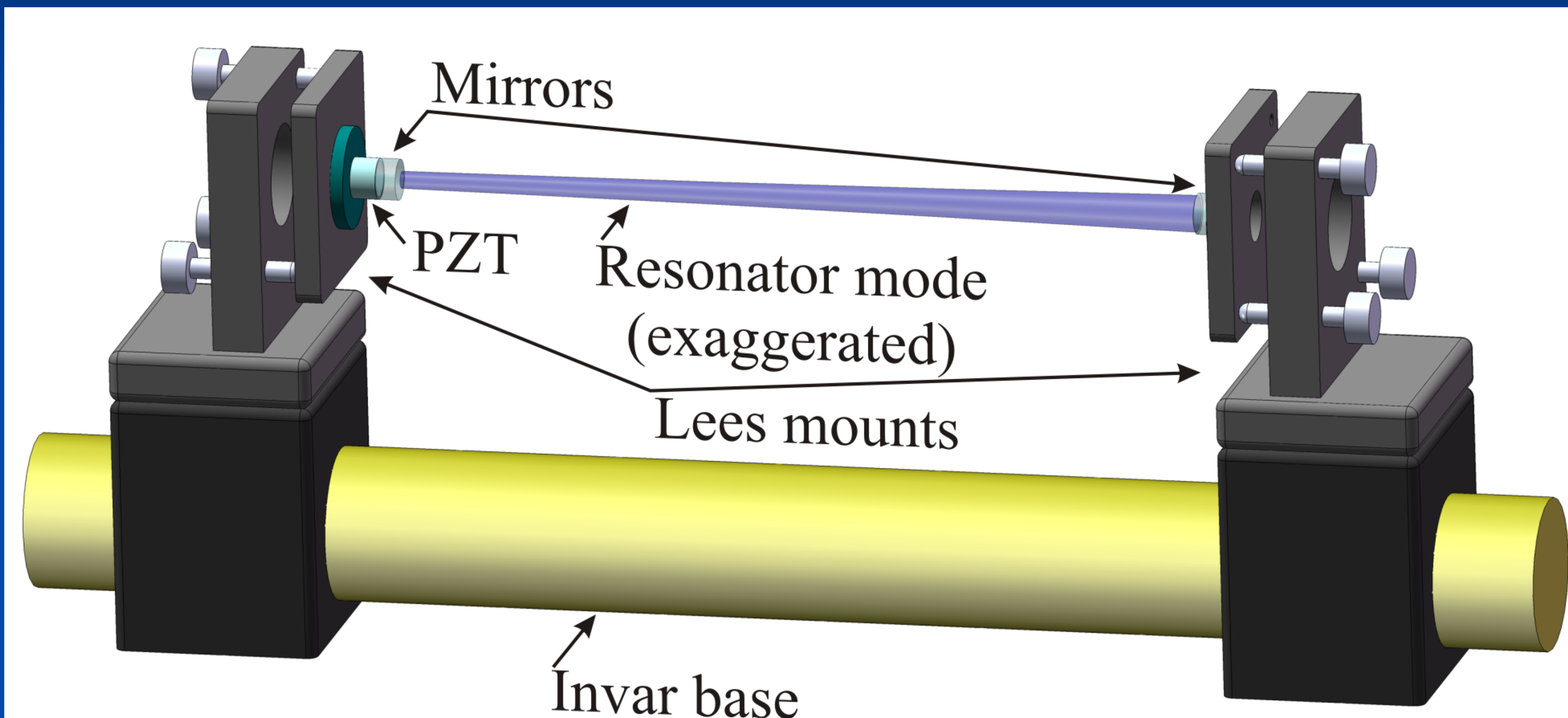

Power-buildup cavity design and characterization

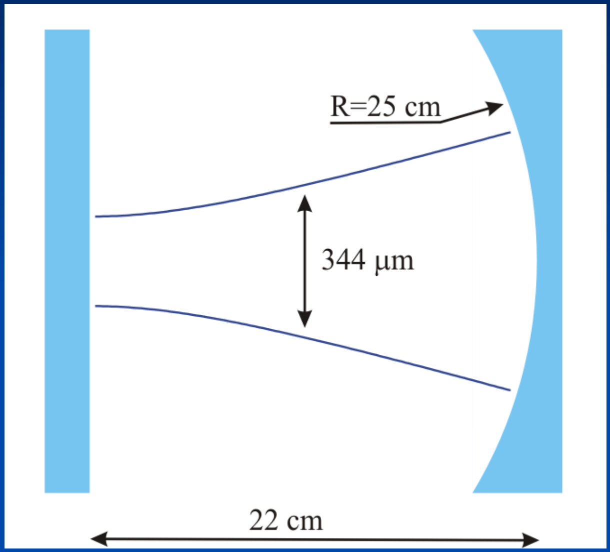

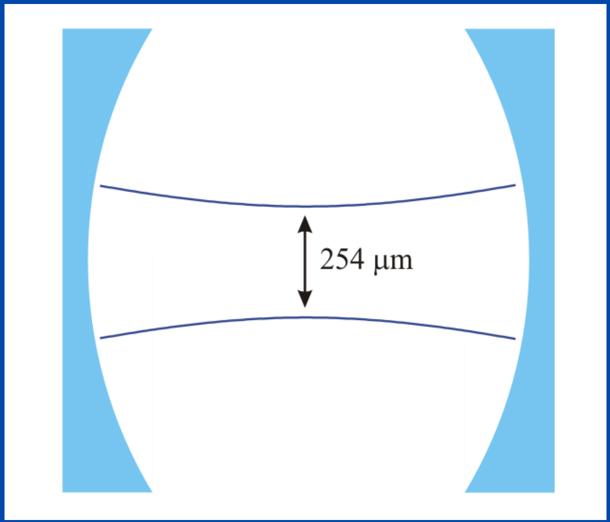

$$F = \frac{2\pi}{T_1 + T_2 + L_1 + L_2}$$

$$\frac{P_{trans}}{\varepsilon \; P_{in}} = T_1 T_2 \left(\frac{F}{2\pi} \right)^2$$

C. J. Hood, H. J. Kimble, J. Ye. PRA 64, 2001

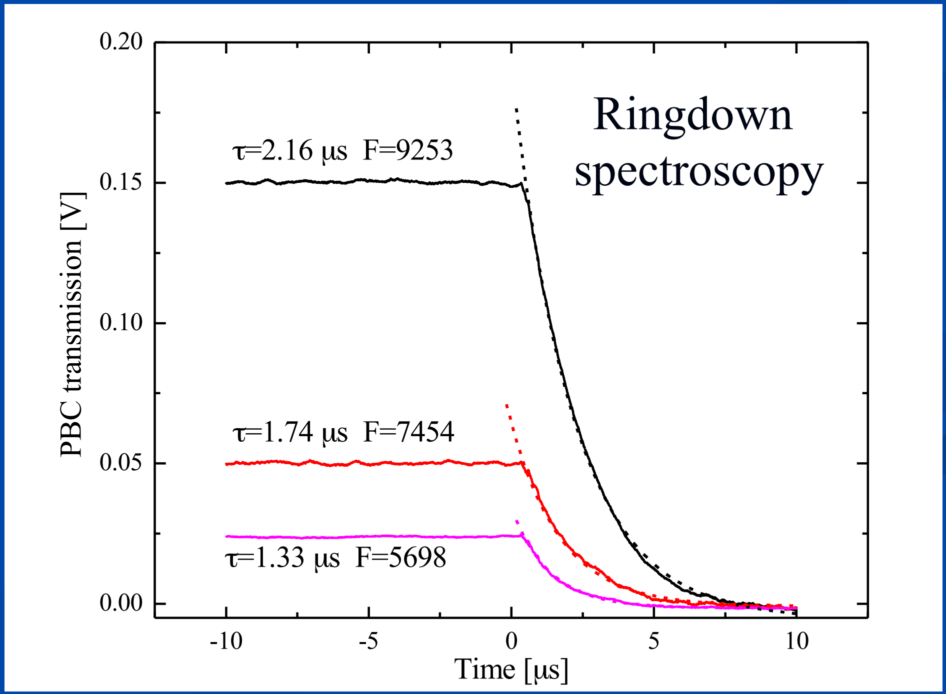

Power-buildup cavity design and characterization: mirrors

	REO set1 λ=408 nm	REO set2 λ=408 nm	ATF λ=408 nm	Boulder expt. λ=540 nm
Transmission	320 ppm	45; 23 ppm	150 ppm	40; 13
S+A losses	120 ppm	213; 83 ppm	30 ppm	<1 ppm

Mirror set used during the latest APV measurements:

Finesse of 17000 with ATF mirrors

Photodegradation: a factor of 3 increase of S+A losses in 2 runs (~8 hours of exposure with ~10 W of circulating power)

Yb isotopes and abundances

Seven stable isotopes, two have non-zero spin

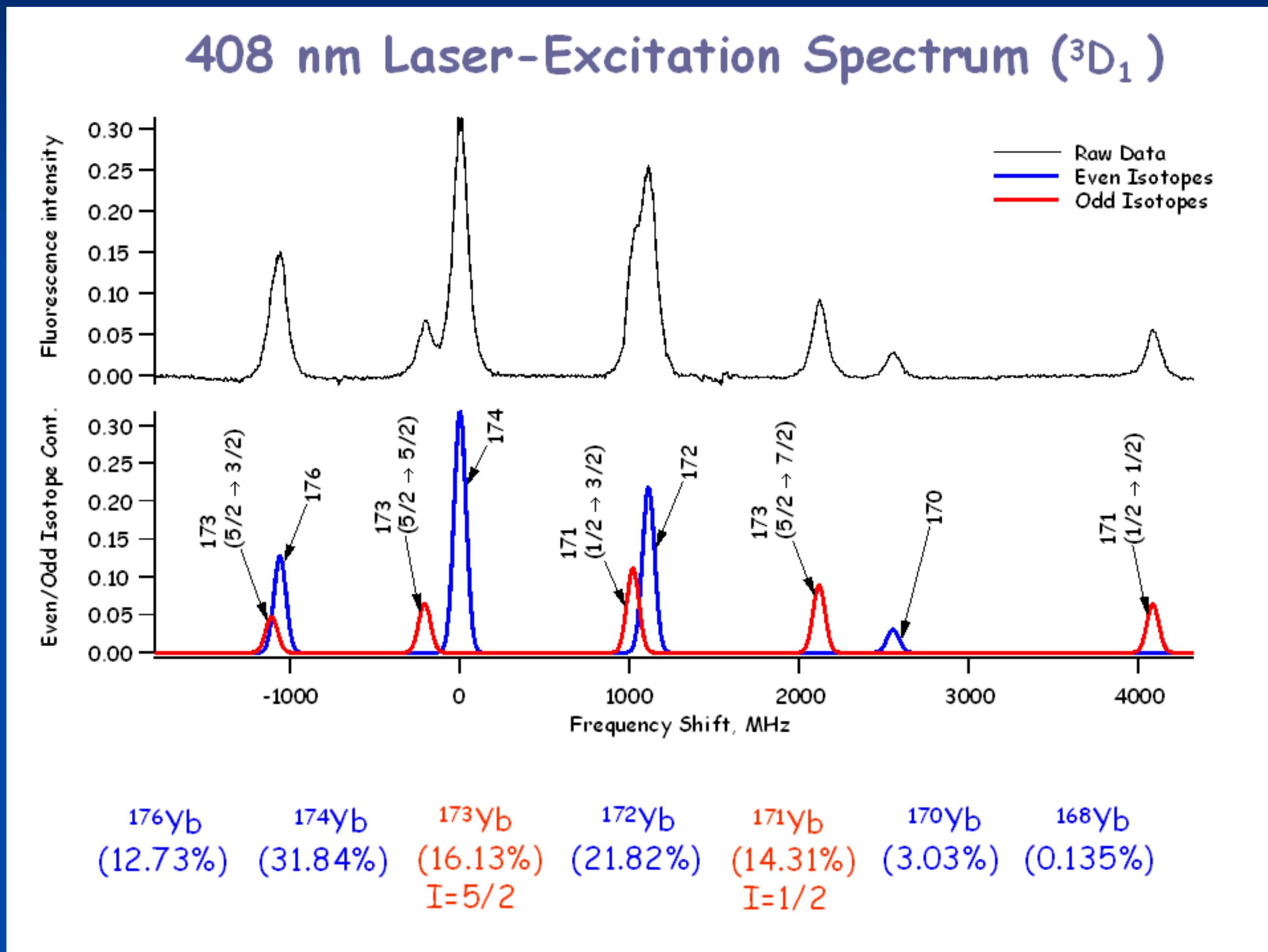

C.J. Bowers et al, PRA 1999

Sources of NSD interaction

$$\hat{h}_{NSD} = \frac{G}{\sqrt{2}} \frac{\kappa}{I} \gamma_0 \boldsymbol{\gamma} \mathbf{I} \; \rho(\vec{r})$$

Anapole moment

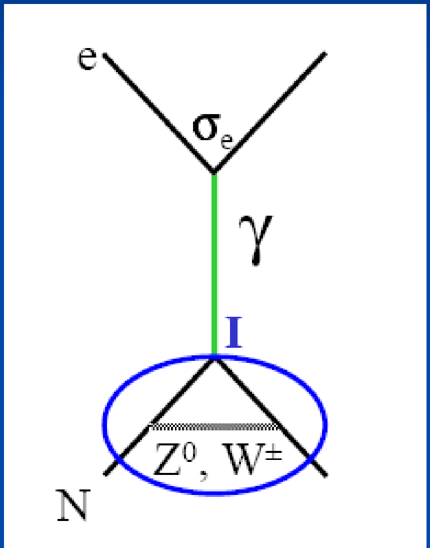

Weak neutral current

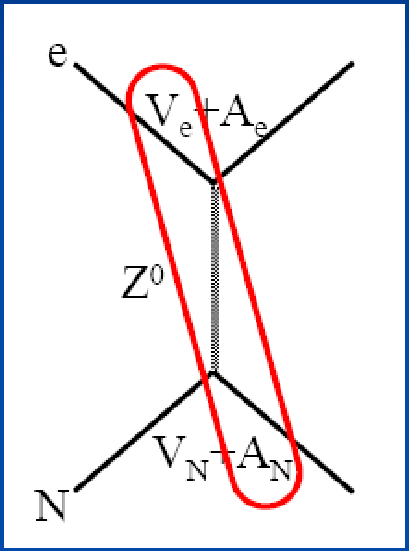

Hyperfine correction to the weak neutral current

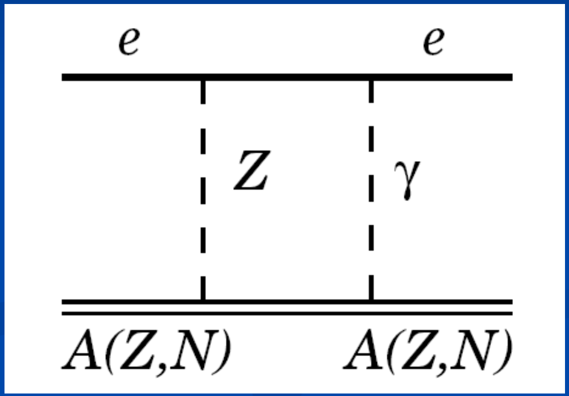

$$\kappa = \frac{K}{I+1}\kappa_A + \kappa_2 + \kappa_{Q_w};$$

$$K = (-1)^{I+1/2-l}(I+1/2)$$

$$\kappa_A \approx 1.15\cdot 10^{-3} A^{2/3} \mu_\alpha g_\alpha; \quad A = N + Z;$$

$$\kappa_2 = \frac{1/2 - K}{I+1} C_{2\alpha}$$

κ_A-Anapole moment
κ_2-Neutral currents
κ_{QW}-Radiative corrections

Anapole moment

In the nonrelativistic approximation PNC interaction of the valence nucleon with the nuclear core has the form:

$$\hat{h}_A \propto \frac{G\, g_\alpha}{2\sqrt{2}} \frac{(\boldsymbol{\sigma}\mathbf{p})}{m_p} n(\vec{r})$$

n(r) is core density and g_α is dimensionless effective weak coupling constant for valence nucleon.

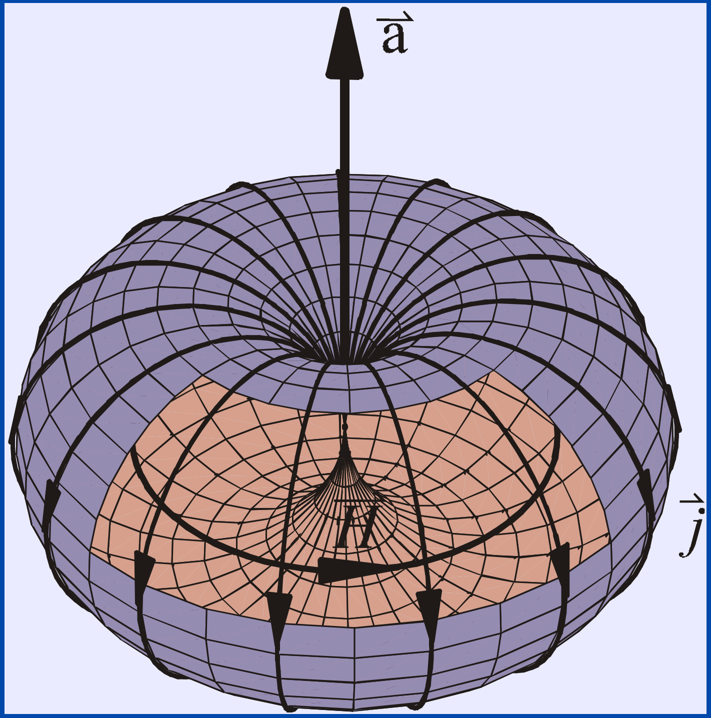

- As a result, the spin σ acquires projection on the momentum **p** and forms **spin helix**
- Spin helix leads to the toroidal current. This current is proportional to the magnetic moment of the nucleon and to the cross section of the core.

Khriplovich & Flambaum

$$\kappa_A \approx 1.15 \cdot 10^{-3} A^{2/3} \mu_\alpha g_\alpha$$

neutron: μ_n=-1.2; g_n=-1

proton: μ_p=3.8; g_p=5

Anapole moment is bigger for nuclei with unpaired proton

Nuclear physics implication: weak meson coupling constants

There are 7 independent weak couplings for π-, ρ-, and ω-mesons known as DDH constants. Proton and neutron couplings, g_α, can be expressed in terms of 2 combinations of these constants:

$$g_p = 8.0\times10^4\left[70f_\pi - 19.5h^0\right]$$

$$g_n = 8.0\times10^4\left[-47f_\pi - 18.9h^0\right]$$

$$f_\pi \equiv f_\pi^1 - 0.12h_\rho^1 - 0.18h_\omega^1$$

$$h^0 \equiv h_\rho^0 + 0.7h_\omega^0$$

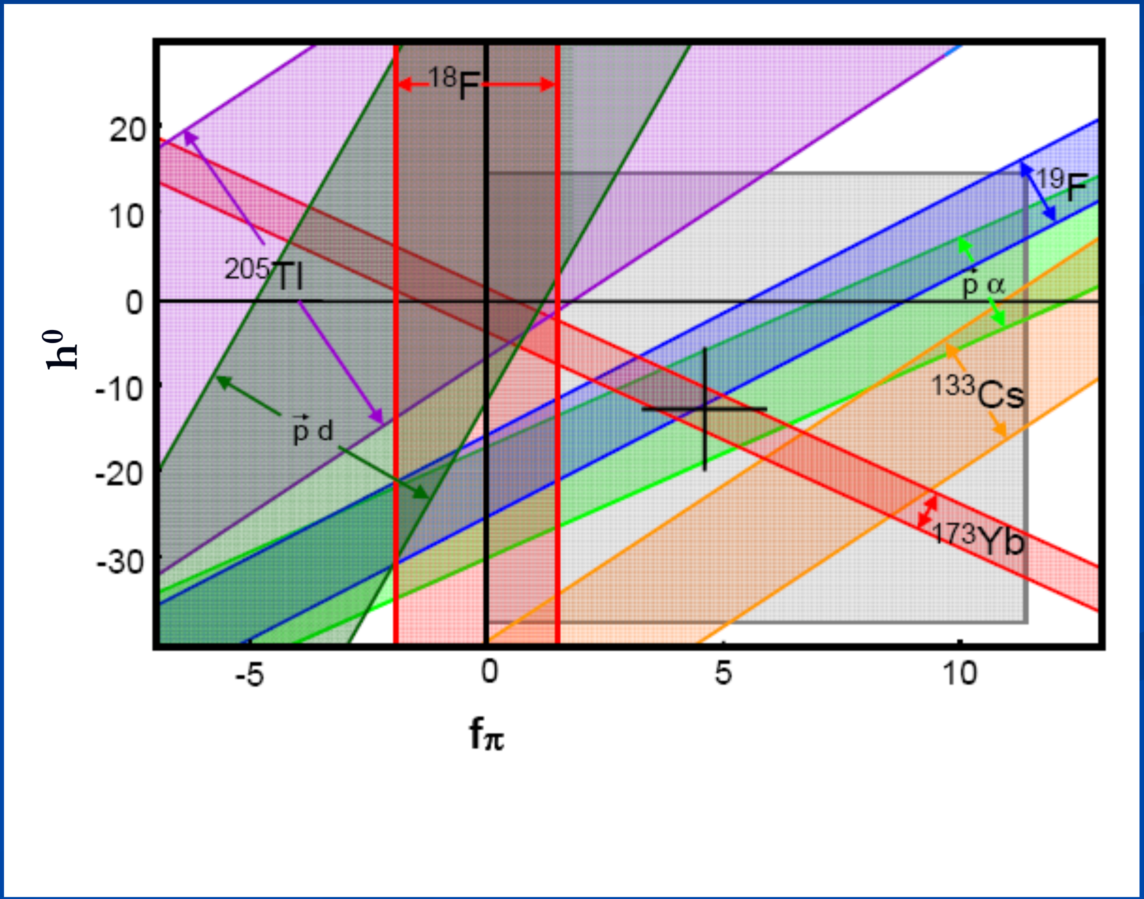

At present the values of the coupling constants are far from being reliably established. The projected measurement of the anapole moment in ^{173}Yb should provide an important constraint.

PV effect on line shapes: odd isotopes

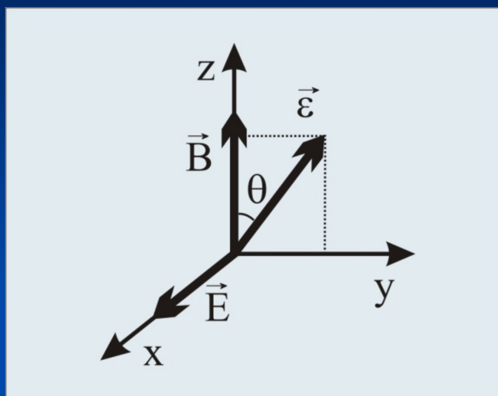

$$\vec{E} = (E,0,0)$$

$$\vec{\varepsilon} = (0,\sin\theta\ ,\cos\theta)$$

$$R^{center} = \frac{\beta_{FF'}^2 E^2}{6}(4\sin^2\theta + \cos^2\theta) + E\ \beta_{FF'}\varsigma'\sin\theta\cos\theta$$

$$R^{side} = \frac{\beta_{FF'}^2 E^2}{2}\cos^2\theta - E\ \beta_{FF'}\varsigma'\sin\theta\cos\theta$$

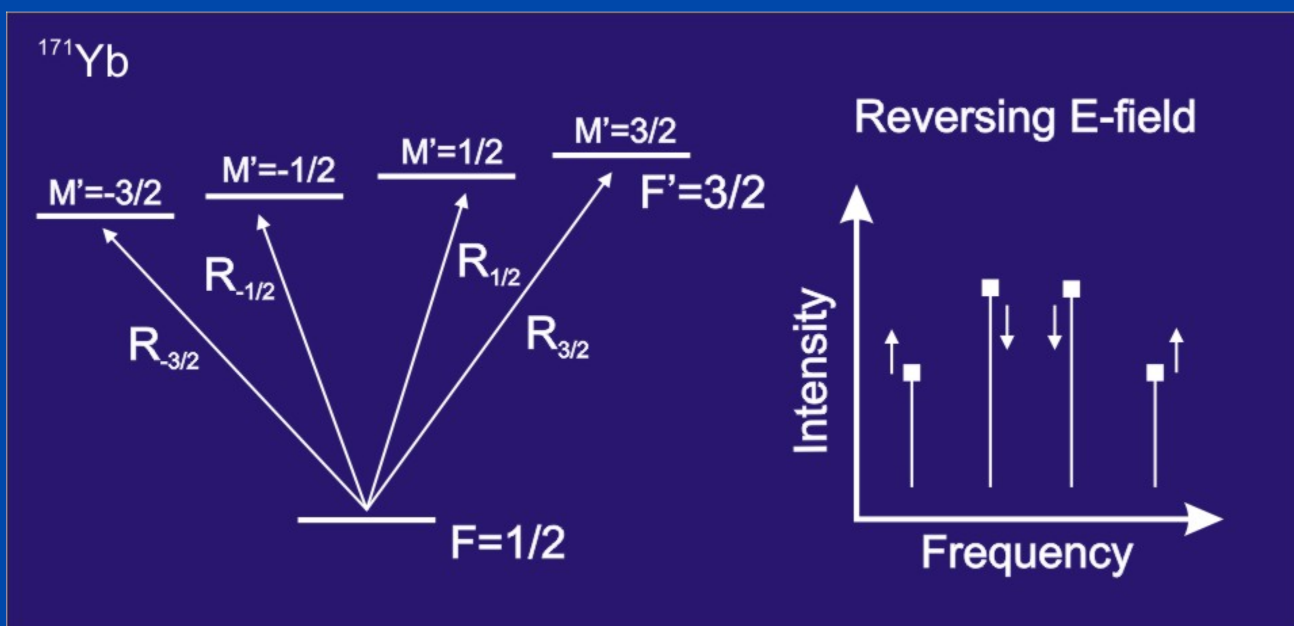

$$\varsigma' = \varsigma + \left\langle \vec{I}\cdot\vec{J} \right\rangle\ \varsigma^{NSD}$$

$\zeta^{NSD} \approx 10^{-12}\ ea_0$ for odd Yb isotopes

$\zeta = 10^{-9}\ ea_0$

ζ` must be measured with 0.1% accuracy